Microfluidic tools for studying coalescence of crude oil droplets in produced water

Marcin Dudek[1], Are Bertheussen[1], Thomas Dumaire[2] and Gisle Øye[1,†]

[1] Ugelstad Laboratory, Department of Chemical Engineering, Norwegian University of Science and Technology (NTNU), Trondheim, Norway

[2] Sorbonnes Universités, UPMC University of Paris 6, Paris, France

† Corresponding author: gisle.oye@chemeng.ntnu.no; Sem Sælandsvei 4, 7491 Trondheim, Norway

ABSTRACT

The major contaminant targeted during the treatment of the oilfield produced water is dispersed oil. The efficiency of most separation processes highly relies on the size of the droplets, which can be increased through coalescence. Crude oil has a complex and field-dependent composition, which can affect the interfacial properties of the drops, and consequently the merging process in different ways. This study focused on the development of microfluidic techniques for investigating coalescence between crude oil drops. The experiments were performed with six diluted crude oils and three neat oils, the latter in the presence of an oil-soluble surfactant. The composition of the water phase was systematically varied (pH, ionic composition, presence of dissolved components). In general, crude oil droplets coalesced more readily in lower or neutral pH. The addition of dissolved Fluka acids to the water phase had a unique effect on each crude oil, reflecting their composition. What is more, this effect was similar to the presence of water-soluble crude oil components in the aqueous phase. The pressure did not have a significant effect on the coalescence, which was explained by the lack of the lightest components (C1-C4) in the system. In summary, the results revealed several trends, however it was clear that the coalescence highly depended on the oil composition. This underlined the necessity for experimental methods, such as microfluidics, which allow for quick assessment of the stability of crude oil droplets.

KEYWORDS

1. INTRODUCTION

During petroleum production, large volumes of water are co-produced with crude oil and natural gas. This produced water (PW) can be composed of formation water, injected fluids (e.g. seawater or production chemicals), dispersed crude oil, solid particles, and dissolved inorganic and organic components. Globally, it is estimated that the produced water to oil ratio is approximately 3:1[1].

Before the produced water is disposed of (e.g. by re-injection to the reservoir or discharge), it has to undergo quality improving treatment. The main contaminant targeted during the produced water treatment (PWT) processes is the dispersed crude oil. The limit for the discharge of the PW to the sea is between 30 and 40 ppm of oil in water (OiW), depending on the local regulation. However, due to increasing environmental concerns, many countries push for even stricter regulations[2]. The 'Zero Harmful Discharge' policy, initiated at the Norwegian Continental Shelf, not only decreases the limit of the dispersed OiW concentration, but also underlines the necessity for targeting dissolved components during water treatment. Re-injection of the produced water can waive the problem of aquatic pollution, as the oily water is pumped back to an underground formation. Moreover, it can also be used as an increased oil recovery technique that sustains the pressure in the production reservoir. Nevertheless, to avoid formation damage, the requirements for the quality of the produced water must be tailored to the reservoir characteristics and can be similar to those for the discharge[3].

A typical offshore produced water system is composed of a bulk gravity separator, a sand handling system, a hydrocyclone and a gas flotation unit (Figure 1).
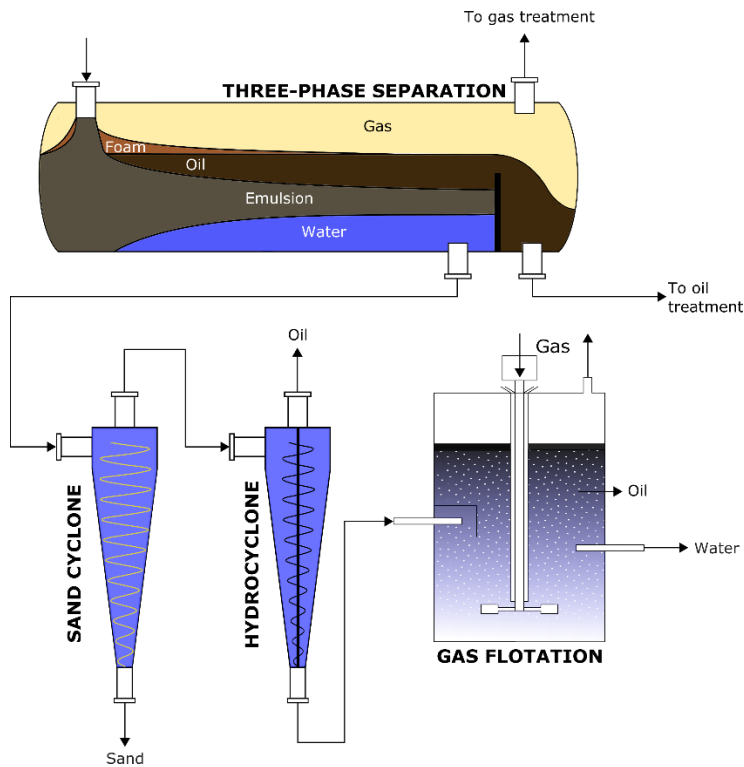
Figure 1 Typical produced water treatment process

The water leaving the gravity separator typically contains 1000 ppm or less of crude oil. The hydrocyclone treatment reduces it further down to 100-300 ppm of OiW, while the gas flotation unit can decrease the oil concentration below the discharge limit. As the oil fields mature, the water cut increases and can reach as high as 95%. Therefore, at some point of the production, the handling of the produced water can bottleneck the entire process. For this reason, subsea treatment of the produced water is considered as a viable alternative to the topside PWT.

Subsea production and processing of crude oil and gas is one of the few options when moving into deeper and more remote waters. In the past two decades, the underwater installations around the world evolved from single satellite wells to complex systems that can perform boosting, compression and separation operations[4]. The subsea treatment of the produced water not only carries the advantage of the reduced volumes of pumped fluids and decreased pressure drop, but can also be beneficial to the separation process. Higher pressure and temperature, maintained in the subsea separation system, can enhance the density difference between the separated phases and

reduce the viscosity of the fluids. As a result, the separation efficiency should be higher subsea, compared to the topside conditions[5].

Most of the produced water treatment processes, such as gravity separation, hydrocyclone or gas flotation, highly rely on the droplet size. As described by Stokes law, the creaming velocity in the gravity separators is directly proportional to the square of the drop diameter. In addition, larger drops are easier to encounter by gas bubbles during gas flotation. With the increase of the drop size, the PWT processes are quicker and more effective, resulting in less dispersed OiW in the discharged or reinjected water.

Coalescence is the main process controlling the droplet growth. It can be split into three steps[6]: (1) droplet approach (and collision), (2) thin film drainage and (3) film rupture and fusion of two drops into one. Since the stability of emulsions is an important aspect of many industrial processes, either as a goal to reach or a problem to overcome, it has been extensively studied for many years. Several studies of the coalescence of model oil-in-water drops had been conducted[7-9]. Regarding the crude oil systems, the researchers have paid more attention to the coalescence of water drops in the continuous oil phase[10-13], leaving the crude oil-in-water systems a relatively unexplored topic[14-15]. In addition, there are hardly any research tools that allow systematically investigating the coalescence of crude oil drops in water.

Crude oil has a very complex composition and can contain a variety of species that influence their interfacial properties, such as resins, asphaltenes[16-17], and acidic species[18]. The dissolved components in the water, partitioned from the oil phase[19], can also adsorb at interfaces[20] and affect the coalescence process. Moreover, crude oil drops may behave differently, when subjected to subsea conditions (i.e. high pressure or temperature). To the best of our knowledge, the effect of pressure on the merging of crude oil drops has not been reported in the literature.

Microfluidics proved to be a very useful tool for studying emulsion stability. Both model oil-in-water[21-23] and water-in-oil systems[24-26] were previously reported in the literature. In the petroleum

science, however, the focus of microfluidic applications is rather shifted towards fluid analysis[27-29] and very few papers concerning separation can be found[30]. <mark>While in microfluidics the effect of gravity is negligible, it still allows to systematically study the merging of drops during flow, in contrast to other techniques that study coalescence in more static conditions[31].</mark>

Previously we have presented a microfluidic approach to study the coalescence of model oil-in-water systems at increased pressure[32]. The objective of the current work was to develop methodology for studying coalescence of crude oil drops under different conditions using microfluidics. The investigated parameters included the composition of the oil phase (different crude oils, diluted and neat), water phase (salinity, pH, dissolved components) and pressure.

2. EXPERIMENTALS

2.1. Chemicals. The physical and chemical properties of six crude oils, produced at the Norwegian Continental Shelf, are summarized in Table 1. Additional characterization (except of crude oil F) and description of methods were reported elsewhere[33].

Table 1 Physicochemical properties of crude oils.

Crude oil		API [°]	Viscosity [mPa s] @20°C	TAN [mg KOH/ g oil]	TBN [mg KOH/ g oil]	SARA [% wt.]			
						Saturates	Aromatics	Resins	Asphaltenes
■	A	19.2	354.4	2.2	2.8	50.6	31.2	15.7	2.5
■	B	35.8	14.2	ND	1.0	84.0	13.4	2.3	0.3
■	C	23.0	74.4	2.7	1.1	64.9	26.3	8.4	0.4
■	D	36.3	10.2	0.2	1.1	71.5	23.1	5.1	0.3
■	E	37.9	8.3	0.5	0.4	74.8	23.2	1.9	0.1
■	F	39.7	7.5	0.1	0.6	78.5	18.9	2.5	0.1

The crude oils were initially diluted to 25% wt. with xylene (Mix of isomers, AnalaR, VWR, USA) to be used as the dispersed phase in the microfluidic investigations. During further tests, three crude oils (B, E, F) were used without dilution and upon addition of 200 ppm of a de-emulsifier. Unless stated otherwise, the measurements were performed with one de-emulsifier (A few experiments in the Section 3.2.1. were also conducted with another de-emulsifier). These additives will later be referred to as oil-soluble surfactants.

Two types of brine were used to simulate produced water salinities at the Norwegian Continental Shelf[34] and to investigate the effect of the divalent ions on the coalescence of the crude oil droplets. Both brines had equal ionic strength (I=0.59M). The first brine, referred to as Na-Brine, contained only sodium chloride (p.a., Merck Millipore, USA). The other, NaCa-Brine, was a mixture of NaCl and $CaCl_2$ (p.a., Sigma-Aldrich, USA) with Ca/Na molar ratio of 1:35. The brines were adjusted to pH 4 and 10 by using solutions of diluted HCl (AnalaR, VWR, USA) and dissolved NaOH (AnalaR, VWR, USA). The natural pH of the brines, later referred to as pH 6, ranged between 5.8 and 6.6. All aqueous solutions were prepared with deionized water (Millipore Simplicity Systems, Darmstadt, Germany).

2.2. Dissolved components. Three kinds of components were dissolved in water and used as the continuous phase in different microfluidic experiments.

2.2.1. *4-Heptyl benzoic acid (4-HBA).* 100 ppm of the 4-HBA (99+%, Alfa Aesar, USA) was dissolved in Na-Brine at high pH. Subsequently, the solution was adjusted to pH 10.

2.2.2. *Fluka acids.* The water phase with a commercial naphthenic acid mixture (Fluka, Sigma Aldrich, USA; later denoted as Fluka acids) was obtained through partitioning. Heptane (HPLC ≥99%, Sigma-Aldrich, USA) containing Fluka acids was poured into Schott bottles with buffered Na-Brine at pH 6 and 9, respectively. After 12 hours of horizontal shaking, the phases were separated by centrifugation (30 min at 11000 rpm). Part of the water was acidified to pH<2 with hydrochloric acid and shaken with pure heptane to back-extract the organic content for concentration measurement. Samples were silanized with N-tert-Butyldimethylsilyl-N-methyltrifluoroacetamide (MTBSTFA) with

1% tert-Butyldimethylchlorosilane (Sigma-Aldrich, USA) and then analysed with GC/MS for quantification. Finally, the samples were diluted with Na-Brine to contain 100 ppm of acids and adjusted to pH 6 and 10, respectively.

2.2.3. *Dissolved components from crude oils.* Each of the crude oils were mixed with Na-Brine at pH 4, 6 and 10 in order to saturate the water phase with water-soluble oil components. Approximately 100 ml of brine and crude oil were poured into Schott bottles and put on a vertical shaker (200 rpm) for 48 hours. Subsequently, the water phase was extracted and centrifuged to remove any dispersed oil. The pH was measured and afterwards readjusted to the original level. Some water phase was collected, acidified to pH<2 with sulphuric acid, and analysed for the total organic carbon content (TOC-L$_{CPH}$ Analyser, Shimadzu, Japan). The measurements were performed at GIG Research Institute in Katowice, Poland.

2.3. Microfluidic chips and setup. The design of the chips and the microfluidic setup is illustrated in Figure 2.
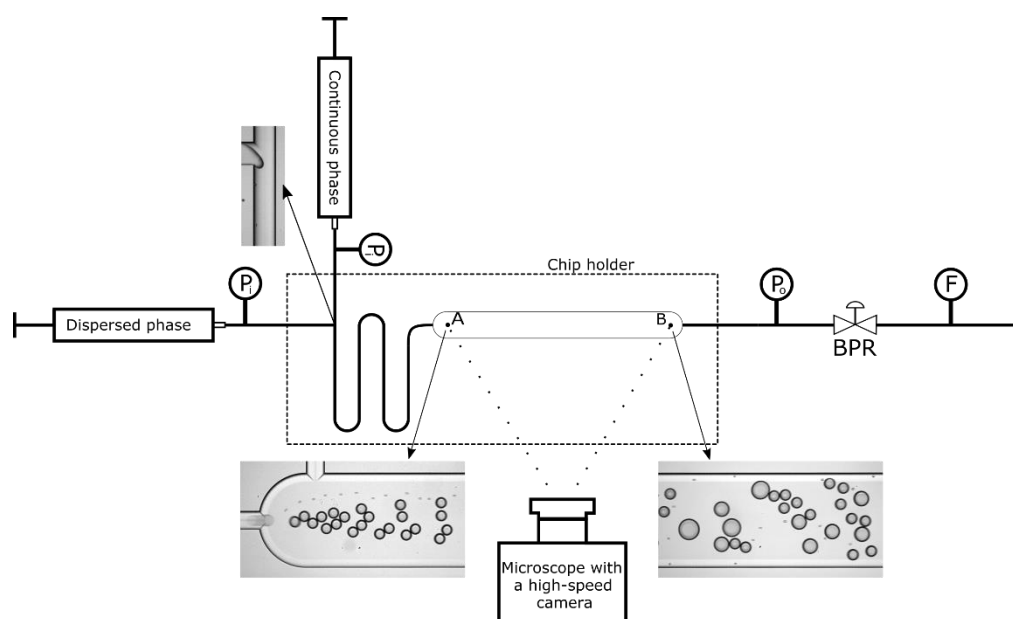

Figure 2 Illustration of the microfluidic setup and chips.

Custom-designed glass microfluidic chips were delivered by Micronit Microtechnologies B.V. (The Netherlands). The inlet channels had a width of 100 μm and led to a T-junction, where the droplets were generated. The drops then passed a meandering channel and entered a coalescence chamber

with the width of 500 μm and length of ca. 33 mm, where they could get in contact and possibly undergo coalescence. The wider channel led to the outlet of the chip. All channels had a uniform depth of 45 μm. During the experiments, the chip was placed in a chip holder (Fluidic Connect PRO, Micronit Microtechnologies B.V., The Netherlands) and connected to the rest of the flow setup with FFKM ferrules and PEEK tubing (inner diameter 250 μm, Sigma-Aldrich, USA). The high-pressure measurements were performed with another chip holder (Fluidic Connect 4515, Micronit Microtechnologies B.V., The Netherlands). After the experiment, the chips were cleaned through sonication in three different solvents: toluene/acetone mixture (3:1 v/v), isopropanol and deionized water. Each cleaning step lasted 15 min. Finally, the chips were dried with compressed air and baked in an ashing furnace for six hours at 475°C. Shortly before the experiments, the chips were treated in low-pressure oxygen plasma chamber (Zepto, Diener electronic GmbH, Germany) for 10 minutes.

The liquids were pumped with syringe pumps (neMESYS mid-pressure module V3, Cetoni GmbH, Germany). The pressure level in the system was controlled by a backpressure regulator (BPR in Figure 2, JR-BPR2, VICI AG International, Switzerland) and monitored with pressure sensor modules (Qmix P, Cetoni GmbH, Germany) at the inlet and outlet of the chip (P_i and P_o in Figure 2, respectively). The flow was measured with a flowmeter (F in Figure 2, mini CORI-FLOW, Elveflow, France). The droplets were observed with a high-speed camera (AX100, Photron, Japan), connected to an inverted microscope (Ti-U Eclipse, Nikon, Japan) with an external LED light source (HDF7010, Hayashi, Japan) at a constant framerate of 8500 frames per second.

2.4. Microfluidic experiment, data acquisition and image analysis.

The experiments were conducted similar to a previous report[32]. In short, the oil and water flow rates were set to 10 and 160 μl/min, respectively. In these conditions the droplets had a diameter of approx. 50 μm. Due to the smaller channels at the inlet of the chip, the readings from the pressure sensor located there indicated approx. 2 bar higher pressure, compared to the outlet of the chip. This pressure drop was present in all tested pressure levels. The Reynolds number inside the

coalescence channel ($Re = \frac{\rho v l}{\eta}$, where ρ and η are the density and viscosity of the continuous phase, v is the velocity and l is the width of the channel) was equal to 50. The Weber number ($We = \frac{\rho v^2 l}{\gamma}$, where γ is the interfacial tension between oil and water), which compares the inertial forces to interfacial tension, in our case was typically below 1. Both Reynolds and Weber numbers are typically low for microfluidic applications[35]. The Capillary number ($Ca = \frac{v\eta}{\gamma}$), describing the ratio of viscous stresses to stresses due to interfacial tension, was in the range of 10^{-2}. Even though both the Reynolds and Weber number were much lower than in a process taking place in a gravity separator, the velocity of the droplets in our system (ca. 0.1 m/s) was comparable to the water flow during the separation process[36].

Two sets of images were taken for each experiment – at the inlet and the outlet of the microfluidic chip (points A and B in Figure 2, respectively). The series from the inlet was used to retrieve the initial size and number of the droplets, and additionally used to verify the accuracy of the recordings from the outlet of the chip. Next, a series of 7000 frames was recorded at the end of the coalescence chamber to assess the extent of coalescence. Both image sequences were processed with the ImageJ software. The frames were first converted into a binary mask and then the areas and the centre of mass coordinates of droplets were retrieved with the Analyse Particle feature. The data was then copied to a Microsoft Excel spreadsheet. It was found that the droplet area increased proportionally with the number of coalescence events. For this reason, the droplets could be sorted into several size classes. It is worth pointing out that the same droplets were detected several times in the consecutive frames. Therefore, the actual number of droplets in each size class (N_f), used for further analysis, was calculated with the average droplet velocity, the width of the detection box and the mean droplet diameter in each size class. The number of initially created droplets (N_{in}) was given by $N_{in} = \sum_{i=1}^{i} n_i * \frac{A_{f_i}}{A_{in}}$, where n_i was the number of class i drops, A_{fi} the area of class i droplets at the outlet of the channel and A_{in} the area of the initially formed droplets. On average, each dataset consisted of 1500 droplets of the original size. The coalescence frequency was the main parameter

for the comparison between different conditions. It was calculated by $f = \left(\frac{N_{in}}{N_f} - 1\right)/t_{res}$, where t_{res}

is the residence time of droplets in the channel (channel length divided by the average drop

velocity). All reported values are an average of three parallels with standard deviation.

2.5. Interfacial tension measurements.

The interfacial tension (IFT) measurements were conducted using a pendant drop tensiometer (PAT-

1M, Sinterface Technologies, Germany). Images of a crude oil drop, immersed in a brine solution

were recorded over time. The measurements lasted 100 seconds. The interfacial tensions were

calculated by fitting the drop profiles to the Young-Laplace equation. All measurements were

performed at room temperature (22°C).

3. RESULTS AND DISCUSSION

3.1. Diluted crude oils

Initially, we tried to use crude oils as is, however they partially wetted and adsorbed to the glass

surface, which prevented droplet generation. Diluting crude oils with an aromatic solvent (xylene)

mitigated that issue, allowing us to study the effect of the crude oil chemistry and water

composition. The coalescence frequencies of the diluted crude oils are illustrated in Figure 3.
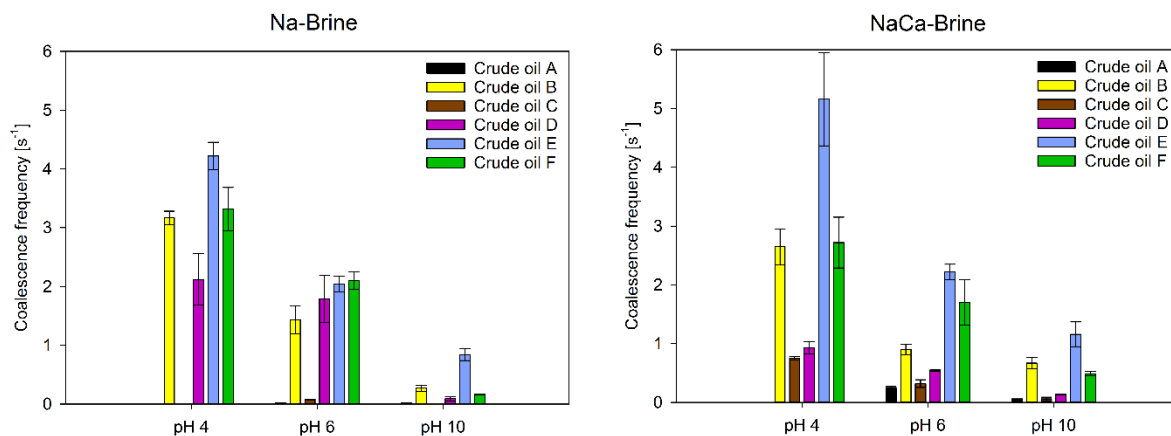

Figure 3 Coalescence frequencies of diluted crude oils in Na- and NaCa-Brine at three pH levels.

In general, the coalescence between the light crude oil drops (B, D, E, F) was more extensive, compared to the heavier ones (A and C). Notably, the viscosity of the oil phases after dilution did not vary much. The final droplet size also depended on the water phase. The highest coalescence frequency was usually observed at the lowest pH and it declined with increasing pH of the water. At low pH, the coalescence between heavier crude oils was difficult to measure, most likely due to the higher TBN values and the fact that in lower pH the glass surfaces often become wetted by crude oils[37] (Figure S1 in SI). In addition, it was impossible to measure the coalescence frequency of crude oil C at pH 10 (Na-Brine) due to the formation very small droplets (Figure S2 in SI), most likely because of high TAN. When calcium was added to the system, the most systematic trend was noticed at pH 10, where its presence boosted the coalescence in almost all cases, compared to the brine without divalent ions. At the other pHs, we did not see any systematic changes in the coalescence frequencies.

Crude oils contain many surface-active components that can be more or less interfacially active in specific conditions. Their interfacial tension (IFT) varies with the pH of the water phase[38]. This is attributed to the presence of protonated basic species at low pH or dissociated acidic components at higher pH. In general, basic components do not lower the IFT as much as the acids, which has been confirmed both for model[19] and crude oil[39] systems. This effect was reflected in the present coalescence studies, where the droplets coalesced more readily in pH 4 or 6. When the pH was increased to 10, the oil-water interface was controlled by the acids and prevented the droplets from merging with each other through increased interfacial concentration of surface-active components. The acidic species in crude oils are often called naphthenic acids. This group includes a wide range of short- and long-chained carboxylic acids, often with aromatic moieties. They can contribute to a variety of undesirable phenomena during the crude oil production, such as emulsion formation, precipitation or corrosion of the pipelines and process units[18]. Due to their amphiphilic nature, they can adsorb at the oil-water interface[38] or even, in the case of low molecular weight compounds, partition to the water phase[40]. Their interfacial activity in neutral or higher pH is probably the main

reason behind the increased stability of droplets. The increase of pH deprotonates more acidic species, which leads to increased interfacial concentration and provides additional stability against coalescence. Moreover, this mechanism is further supported by the results obtained with NaCa-Brine at pH 10. Depending on the molecular structure, naphthenic acids in the presence of an electrolyte in water can form soaps or deposits[41]. These complexes are generally more stable with multivalent ions. High-molecular tetraprotic acids, so called ARN acids, are more likely to form scale[42], whereas low molecular monoacids contribute to forming stable emulsions[43]. In the case of water-in-crude oil emulsions, the latter naphthenates can agglomerate at the interface and lead to problems in flow assurance or separation process[44]. In the case of oil-in-water emulsions, however, it is likely that the addition of calcium removed acids from the interface. These acid-calcium complexes are less interfacially active and more lipophilic in character, which facilitates their diffusion from the interface to the oil phase[45], reducing their interfacial concentration and most likely leading to the increased coalescence.

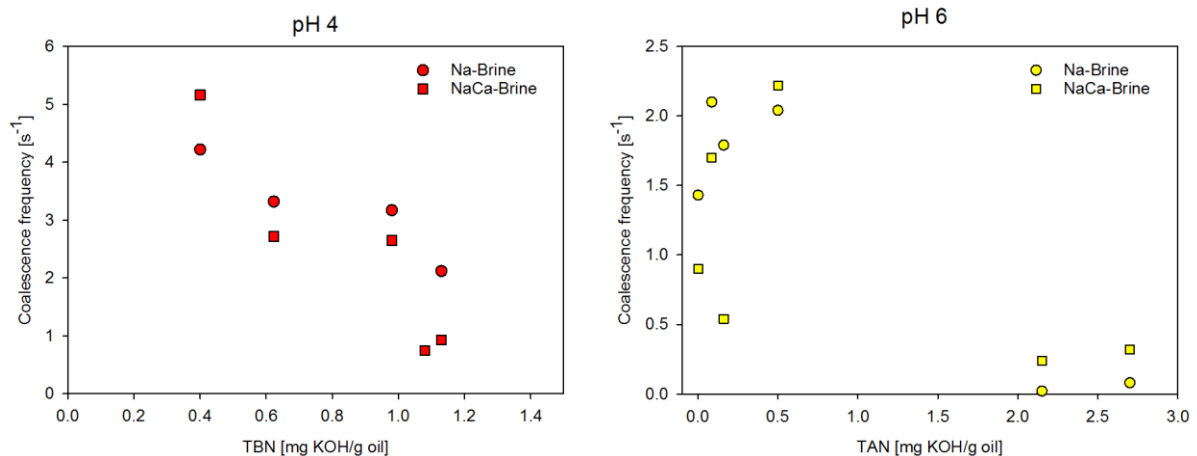Figure 4 depicts the coalescence frequencies plotted against TAN and TBN values.

Figure 4 Coalescence frequencies of diluted crude oil plotted against TBN (left) and TAN (right) values of crude oils. The order of crude oils from left to right: E, F, B, C, D (TBN) and B, F, D, E, A, C (TAN).

The crude oils used in this study had the total base numbers ranging from 0.4 to 2.8. At pH 4, the coalescence frequency was found to be inversely proportional to the TBN of the crude oils. This

effect was similar for both brines. The total base number is traditionally considered as an indicator for the basic species in crude oils. At lower pH, these components become protonated and affect the interfacial properties of the crude oil drops[39]. This effect can depend both on the type of the basic components and their concentration, as observed in our case.

The coalescence behaviour at higher pH was better explained with the total acid number values, as the interfacial properties of crude oil drops are governed by the acidic species. At pH 6 and 10 in Na-Brine, the crude oils could be divided into two groups (plot for pH 10 in Figure S3 in SI). Crude oils with lower TAN value (<0.5) coalesced quite extensively, while hardly any coalescence was observed for the crude oils with high TAN values (>2). This effect can be probably related to the concentration of the acidic species in the crude oils. At pH 6 only the crude oils with TAN value equal to or higher than 0.5 (A, C, E) experienced an increase of coalescence when calcium was present in the water phase. Firstly, it was entirely possible that the interfacial concentration of the naphthenic acids in the less acidic oils might have been too low to observe the effect of calcium. Secondly, the type of acidic components and the extent of dissociation at the oil-water interface could have also played a role[46-47]. At pH 10, significantly more acids were dissociated, which lead to an increase of coalescence upon addition of calcium, based on the mechanism outlined above. At low pH, the surface charge of oil drops was probably close to neutral or even slightly positive[37, 48]. The addition of calcium ions might have increased the positive charge at the surface through induced dipole-ion interactions between the non-dissociated acidic chain and the cation[49], resulting in increased repulsive forces and lower coalescence in most cases. However, it should be stated that each crude oil has a unique composition that will affect the charge of droplets at given pH. If the acids in the oil have a low pK_a, then even at low pH the coalescence might increase, as was the case for crude oil E.

A trend was also observed when the coalescence frequencies were plotted against the sum of resin and asphaltene weight fractions of the crude oils (Figure 5).
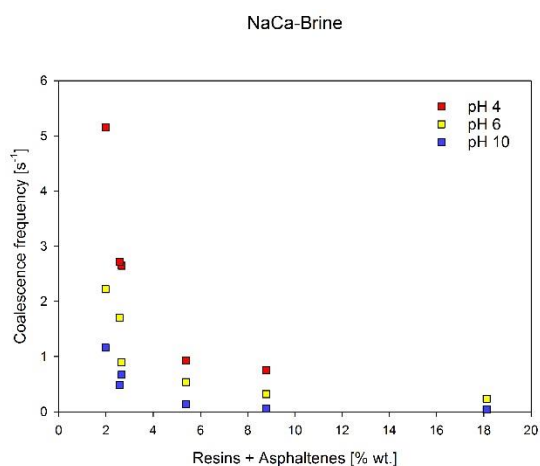
Figure 5 Coalescence frequencies of diluted crude oils plotted against the sum of resins and asphaltenes of respective crude oils.

The coalescence frequencies decayed exponentially with the increasing total resin and asphaltene weight fractions of the crude oils. The coalescence of crude oils with the lowest concentration of these fractions was quite extensive, whereas very little merging occurred at the highest amounts. These trends were similar regardless of the pH or ionic composition (Figure S4 in SI).

The majority of the interfacially active molecules can be found in the resin and asphaltene fractions, which explains their significance for the coalescence frequency. The presence of these species can affect the coalescence between oil drops in several ways. First, the dissociated, charged groups can create electrostatic repulsion, analogous to the effect of ionic surfactants. However, in our system this type of repulsion was significantly decreased due to high electrolyte concentrations. Secondly, the approach and collision between drops may cause gradients in the interfacial concentrations. This will cause a flux of surface-active molecules in the opposite direction of the film drainage process (Marangoni effect), which will impede drainage. Notably, the crude oils were diluted with an aromatic solvent, which effectively eliminated any asphaltene solubility issues. Nevertheless, asphaltenes in a good solvent could still be present as nanoaggregates[50] and impact the formation of viscoelastic films, and subsequently influence the coalescence between oil drops. In general, the emulsion stability is enhanced with the increase of the elastic properties of the interface[51]. Solutions

15

of asphaltenes in aromatic solvents typically exhibit a maximum of elasticity at a certain concentration[52-53]. In our case, the decreasing coalescence frequency with increasing weight fraction of resins and asphaltenes could also be seen for the increasing percentage of asphaltenes alone (Table 1).

3.2. Crude oils

Method development revealed that the addition of an oil-soluble surfactant facilitated the droplet generation process for some of the crude oils without the need of dilution. Therefore, three light crude oils (B, E, F) were used to investigate the effect of the water composition on the coalescence of *non-diluted* crude oil drops.

3.2.1. Water phase effect.

Figure 6 depicts the coalescence frequencies for the non-diluted crude oils in different brines.
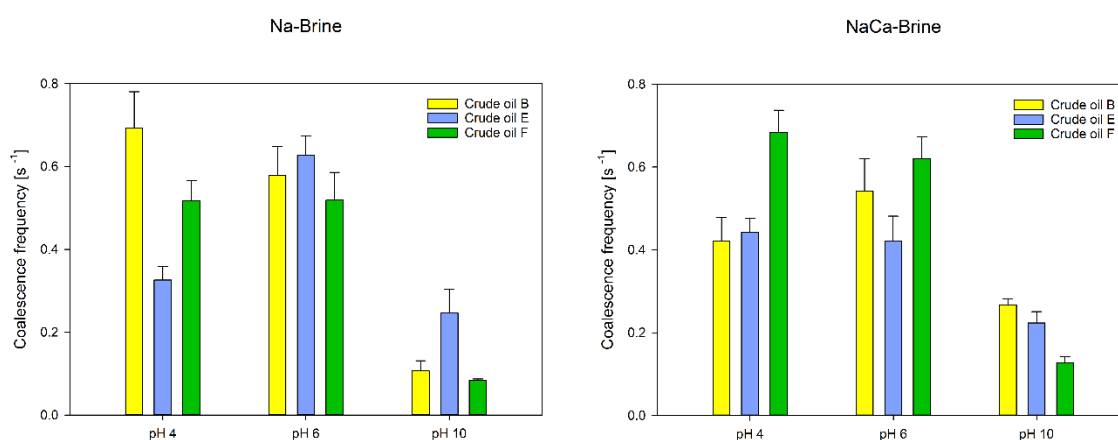

Figure 6 Coalescence frequencies for three crude oils in Na- and NaCa-Brines at different pH levels.

Notably, all coalescence frequencies were significantly lower than for the diluted crude oils. In both brines, the highest coalescence frequencies were observed at pH 4 or 6, and the lower values at pH 10. When considering the effect of divalent ions at pH 10, the coalescence was either higher (B, F) or did not change (E) upon the addition of calcium. The effect of calcium at other pH varied with the crude oil type.

The complex composition of crude oils will definitely have an impact on the coalescence process during the produced water treatment. Like in the Section 3.1, we attempted to connect the crude oil physical and chemical properties to the observed coalescence behaviour. In this case, however, the addition of the oil-soluble surfactant affected the interfacial behaviour of the crude oil droplets, rendering any analysis based on composition unclear. In general, crude oils react differently to various types and concentrations of oil-soluble surfactants. This was confirmed by the experiments performed with another oil-soluble surfactant (Figure S5 in SI). Nevertheless, the trends observed upon changing the water composition remained quite similar to the results obtained with the diluted crude oils.

3.2.2. Dissolved components – model systems.

Certain components of crude oils are water-soluble. Their partitioning to the water phase can occur in the geological formation, where the two phases spend millions of years in contact, and additionally during the production process, where pressure drops and turbulent flow create further opportunities for mixing and mass transfer. Especially the water pH will affect the partitioning in crude oil systems[54]. The concentration of the dissolved components is highly field-dependent, but it can reach several hundreds of ppm in the discharged PW[55]. These components can be toxic and pollute the marine environment[56]. Furthermore, they can affect the oil-water separation process. Our group has previously demonstrated the effect of the dissolved components on the air-water interface[20, 57-58] and the flotation performance[59]. In this section we discuss their influence on the coalescence between crude oil droplets.

The results of the coalescence frequency in Na-Brine with and without the partitioned naphthenic acids at pH 6 is shown in Figure 7.
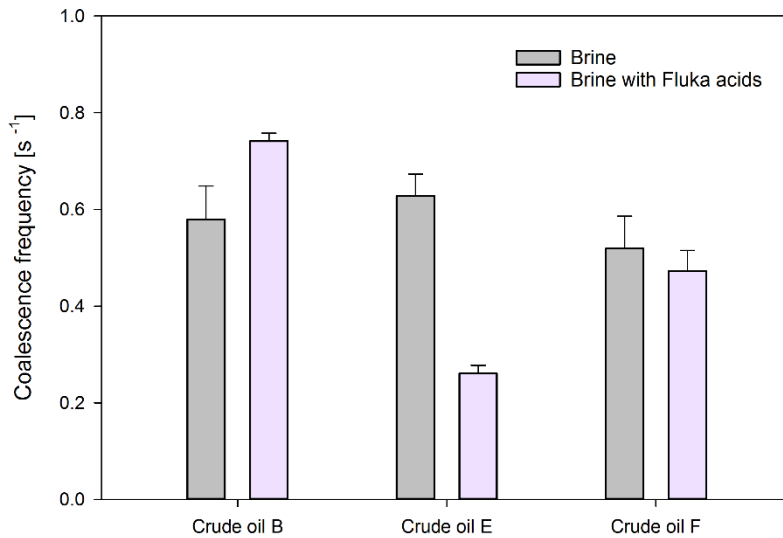
Figure 7 Coalescence frequency of Na-Brine at pH 6 with and without partitioned Fluka naphthenic acids.

Each of the crude oils reacted uniquely to the presence of the dissolved components in the water phase. An increase of coalescence was observed for crude oil B, while the opposite effect was noticed for crude oil E. The dissolved components had little effect on the coalescence with crude oil F. Similar results were obtained for the Fluka acids partitioned at higher pH, presented in Figure 8, together with the results for the 4-heptylbenzoic acid. Also in this case the effect of the dissolved Fluka acids was crude oil-dependent. The acids either promoted coalescence (B, slight increase in F) or reduced it (E).
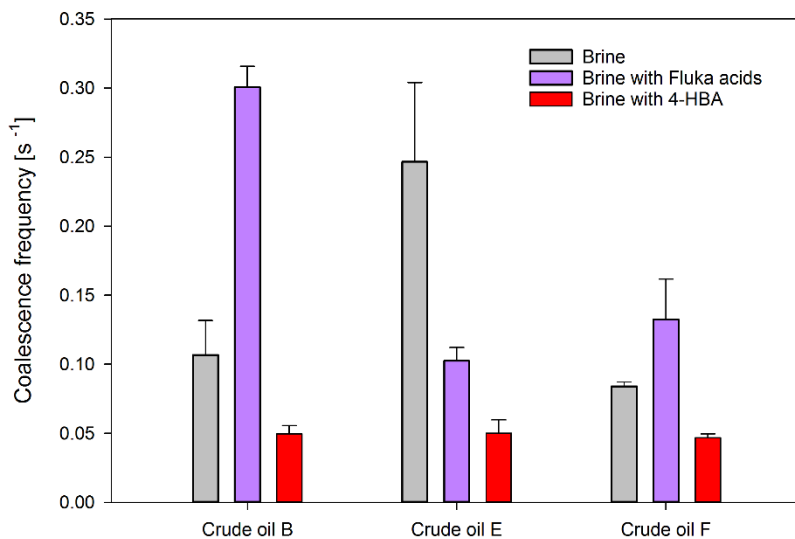
Figure 8 Coalescence frequency of Na-Brine at pH 10 with Fluka partitioned acids, dissolved 4-HBA and without any dissolved components.

Noteworthy, all the oils reacted in a very similar way to the presence of 4-HBA in the continuous phase. The coalescence frequency was reduced to almost identical values of 0.05 s^{-1}, meaning approximately 20 coalescence events for more than 1500 droplets during the recording time.

One possible explanation for the oil-specific response to the presence of the dissolved components is the oil composition, or more precisely the nature of the surface-active components in the crude oils. In the diluted system, crude oil B had lower coalescence frequencies than the other oils. It also had lower resin to asphaltene ratio (R/A) and less aromatic components. Resins are the most polar fraction that is soluble in aliphatic solvents. Although surface-active, they cannot stabilize emulsions by themselves[60]. They are, however, crucial in the emulsion stabilization mechanisms provided by the asphaltenes. Resins were found to increase the stability of asphaltenes in crude oils through solvation[61], and their weight ratio to asphaltene in crude oils correlates inversely with the water-in-oil emulsion stability[60, 62]. Additionally, the R/A ratio has an effect on the film rigidity, which also corresponds to the stability of emulsions[63]. Furthermore, the low fraction of aromatics can contribute to destabilization of asphaltenes. Crude oil B hat the lowest R/A ratio (ca. 8) and lowest

aromatic weight fraction. This might have affected the stability of asphaltenes and increased the film

rigidity in the system with standard brine. Upon the addition of dissolved acids, the less stable

asphaltenes might have been replaced by the smaller acidic species, diffusing from the water phase,

at the interface. Short-chained acids that partitioned at pH 6 might not retard the coalescence

between drops to the same extent as the polar, high-molecular weight components from crude oil B.

In addition, crude oil B has also slightly higher viscosity, which reduced the diffusion rate from the oil

phase to the interface. In the case of crude oil E and F, the smaller amount of more stable

asphaltenes (R/A values of 19 and 25, respectively) should have less effect on the coalescence

process. While there was hardly any difference in the coalescence behaviour for crude oil F, the

crude oil E experienced a significant decrease of coalescence in the presence of the dissolved acids.

Taking the TOC values from Table 2 into consideration, it could be noticed that crude oil F had

almost twice as much components that partitioned to the water phase as crude oil E. Moreover,

these were predominantly short-chained acids, as the decrease of pH from the initial pH 6 value was

much more substantial for that crude oil. Therefore, a competitive mass transfer probably took place

between the short-chained acids coming from bulk oil and the acidic species diffusing from the

water phase. Even though crude oil E has the highest TAN, it probably contains larger acidic

molecules that will diffuse more slowly and will be replaced at the interface by the more mobile

short-chained Fluka acids. In addition, it could be possible that some of the acidic species in the

water phase partitioned into the oil droplet. Groothuis and Zuiderweg[64] stated that the decreased

coalescence rate was expected in systems where mass transfer occured from the continuous to the

dispersed phase. These observations were later confirmed by other groups, who reported that the

direction of mass transfer affected the film drainage time[65]. This phenomenon is often explained

with the Marangoni effect. If the mass transfer occurs from the dispersed to the continuous phase,

the concentration of the transferred solute in the thin film region is increased, which will often

decrease the local interfacial tension. The interfacial tension gradient will facilitate movement of the

fluid outside of the film region, thus promoting film drainage[66]. Conversely, mass transfer from the

continuous to the dispersed phase will retard the drainage process by pushing the liquid into the thin film region. In our case, the mass transfer from the water phase to the crude oil E droplet might have inhibited coalescence, compared to the standard brine. Crude oil F contained more water-soluble acidic components, which possibly limited the mass transfer to the oil phase at pH 6, and did not affect the coalescence in the same way.

Interestingly, the dissolved Fluka acids at pH 6 did not influence the interfacial tension of crude oils (Table 2).

Table 2 Interfacial tensions of crude oils against different water phases. *value reported after 50s; †value reported after 10s. The shorter measurements were due to instability of the generated drop.

Brine type		Na-Brine			NaCa-Brine			Dissolved components		
Oil phase↓	pH→	4	6	10	4	6	10	6 (Fluka)	10 (Fluka)	10 (4-HBA)
Crude oil B		14.9	14.1	6.2*	14.6	13.8	8.7	13.5	4.9	3.8†
Crude oil E		14.9	12.9	9.1	12.8	13.1	10.9	13.5	7.9	4.5†
Crude oil F		6.0*	5.6*	5.8†	5.7*	5.8*	5.6*	5.6*	4.7†	-

The oil-soluble surfactant significantly changed the interfacial properties of the oils. The values without the surfactant ranged from 12 to 22 mN/m (for precise values, please refer to our previous report[33]). In some cases, the drop could not be held for longer than 50 or even 10 seconds. Nevertheless, some trends can be observed. At low and neutral pH, the interfacial tension was almost identical, even when using the brine with Fluka acids. Crude oil F had similar values, regardless of the composition of the water phase. For the two other oils, the IFT at pH 10 was lower. However, it increased upon the addition of calcium, which agrees with the previously proposed mechanisms for the calcium – naphthenic acids interactions. The values of the interfacial tension at pH 10 were somewhat lower when Fluka acids were present, whereas the detection limit (ca. 5 mN/m) of the instrument was reached within 10 seconds after generating the droplet for the brine with 4-HBA. The distributions of Fluka acids are depicted in Figures S6 and S7 in SI.

In all cases, Fluka acids at pH 6 had no effect on the interfacial tension and in the same time affected the coalescence frequency in different ways. This might indicate that their limited surface-activity

could have played a role in either increasing the coalescence frequency by replacing some of the high-molecular weight molecules in the case of crude oil B or decreasing it through diffusion from the continuous phase to the oil phase in the case of crude oil E. Finally, all the crude oils experienced a universal drop of coalescence frequency when 4-HBA was in the water phase. At this high pH, 4-heptylbenzoic acid has very high affinity to the oil-water interface[67], significantly reduces the IFT and stabilizes the droplets against coalescence. The 4-HBA completely filled the oil-water interface and 'neutralized' the indigenous surfactants. In contrast to the polydisperse species in the Fluka acids solutions, the 4-heptylbenzoic acid is a single molecule, that packed more efficiently at the interface.

3.2.3. Dissolved components – water-soluble crude oil species.

Table 3 shows the total organic carbon and pH (before readjustment) after 48 hours of contact between the crude oil and water.

Table 3 TOC and pH values of water after contact with crude oils.

Initial pH	Crude oil B		Crude oil E		Crude oil F	
	TOC [ppm]	pH	TOC [ppm]	pH	TOC [ppm]	pH
pH 4	21	4.33	31	4.93	52	4.07
pH 6	17	5.90	30	6.03	49	4.61
pH 10	21	8.91	33	8.67	52	7.21

The amount of the organic content that partitioned from the oil to the water phase depended on the oil, but also differed slightly with the pH. In some cases, the change of pH after mixing was quite significant, which indicated the nature of the partitioned components. In all cases, the lowest amount of TOC was obtained for the neutral pH, while the most marked pH changes were observed at the highest pH. The water phase from crude oil B contained the smallest amount of dissolved organics and experienced relatively small changes of pH, indicating high molecular weights of both acidic and basic species. Similar observations can be made for crude oil E, with a small exception at pH 4, suggesting the presence of smaller basic molecules, which is supported by the significant decrease of coalescence at that pH for that oil. Brines after mixing with crude oil F contained twice

the amount of the detected organic carbon compared to other oils, and experienced significant

decreases of pH at pH 6 and 10. This implied significant amount of short-chained acids.

The coalescence frequencies in the water phase containing dissolved crude oil components are
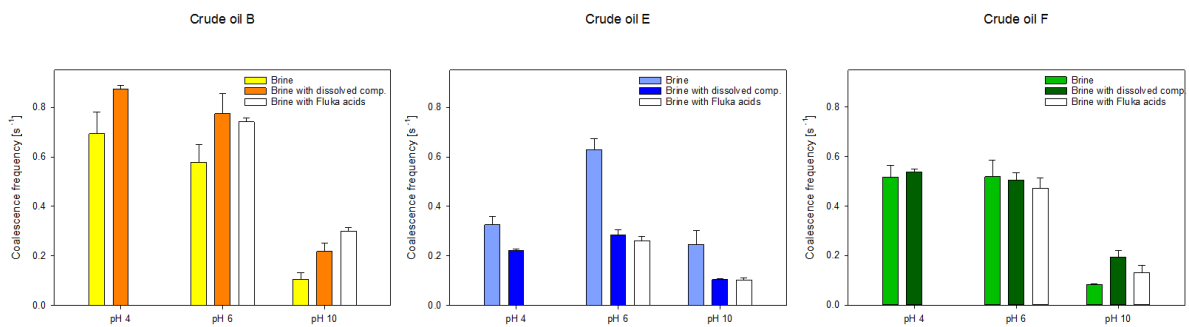
illustrated in Figure 9.

Figure 9 Coalescence frequency of different crude oils in Na-Brines with dissolved crude oil components and Fluka acids.

Also here, the values were oil-specific. The presence of any dissolved components generally resulted

in increased coalescence for crude oil B. The opposite effect was observed for crude oil E, while

crude oil F experienced only minor changes in coalescence behaviour, limited to the highest pH.

Remarkably, the results for the brines with dissolved crude oil components resembled the values

acquired with the water phase containing Fluka acids (white bars in Figure 9).

Water-soluble crude oil species are not only of growing environmental concern, but can also affect

some aspects of the PW treatment processes. There was no correlation between the crude oil

properties and the amount of dissolved organics in the water phase. Moreover, the concentration of

the dissolved components did not affect the coalescence frequency in any systematic way. The

biggest effects were observed for crude oils B and E, which water phases contained significantly less

TOC compared to crude oil F. The results were very similar to the ones presented in the Section

3.2.2., so the previously discussed effect of the dissolved components on the coalescence process

also applies here. Since our study was performed with only three crude oils, it is difficult to

unambiguously state the impact of the dissolved components on the coalescence process. However,

the results demonstrate that their presence in the produced water cannot be neglected. It should

also be noted that the striking similarity of coalescence between the water-soluble crude oil components and Fluka acids suggests that the majority of surface-active components affecting coalescence has acidic nature.

3.2.4. Pressure

Two oils and brines were chosen for experiments at elevated pressure conditions. The results are depicted in Figure 10.
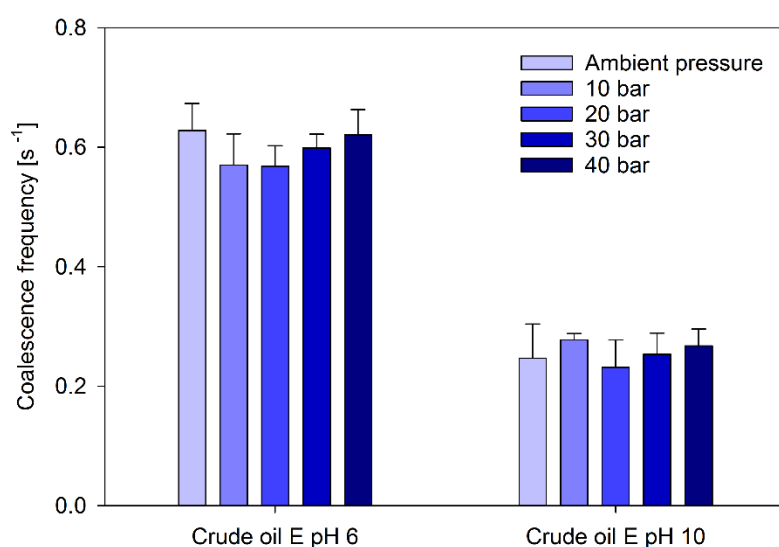

Figure 10 Coalescence frequencies for crude oil E in Na-Brines pH 6 and pH 10 at elevated pressures.

The results show that in the tested pressure range, the extent of coalescence between oil droplets was relatively similar, independent of the pH of the brine and the crude oil (data for crude oil F shown in Figure S8 in SI). The data analysis proved that the differences between the values were statistically insignificant (t-Student, $\alpha=0.05$).

During the course of experiments, we used 'dead' crude oils, meaning that the samples were depressurized and stored at ambient conditions. As a result, the samples were missing the lightest components (C_1-C_4) that usually flash off during depressurization. This means that, in this range, pressure had minor effect on the physical properties of the crude oils[68-69]. Increased system pressure

would lead to increased solubility of the shortest hydrocarbons in the crude oil. This would have several effects on the sample, such as decrease of density or viscosity, and change in the interfacial tension. Higher pressure and change in the crude oil composition can also affect other phenomena associated with crude oil, for instance wax crystallization[70] and asphaltene behaviour[71], which can cause further variations in the oil-water interface and alter the coalescence between drops. Nevertheless, our results showed that the drop fusion remained unaffected by the increased system pressure, showing that the pressure factor will only contribute to the changes in the chemistry of crude oil drops and not influence the mechanisms of the coalescence process.

4. CONCLUSIONS

We have presented microfluidic methods for investigating coalescence between crude oil drops in water phase. The experiments were first performed with diluted crude oils, followed by a study conducted on crude oil drops with the addition of an oil-soluble surfactant. It was demonstrated that both the composition of the oil and water phases influenced the extent of coalescence in our systems. We have also shown that the dissolved components in the water phase can play a crucial role in the merging process and that this effect is likely to be oil-specific. Furthermore, amongst the various water-soluble components from crude oils, the effect of the acids is dominant in the interfacial behaviour of crude oil drops in water. The pressure did not affect coalescence in any way, which was attributed to the lack of light components (C1-C4) in the crude oils.

We believe that the microfluidic coalescence tool in the present paper will help understand the role of crude oil chemistry in the produced water treatment, and become a useful method for probing the stability of crude oil drops in water. With this paper we aimed to present the applicability of microfluidics to the produced water field and its certain advantages over the other available methodologies. With the knowledge on how different parameters affect coalescence of oil drops, the treatment process can be adjusted to promote droplet growth, leading to more efficient

ACKNOWLEDGMENTS

REFERENCES

1.   Fakhru'l-Razi, A.; Pendashteh, A.; Abdullah, L. C.; Biak, D. R.; Madaeni, S. S.; Abidin, Z. Z., Review of technologies for oil and gas produced water treatment. *J. Hazard. Mater.* **2009,** *170* (2-3), 530-51.

2.   Igunnu, E. T.; Chen, G. Z., Produced water treatment technologies. *International Journal of Low-Carbon Technologies* **2014,** *9* (3), 157-177.

3.   Bader, M. S. H., Seawater versus produced water in oil-fields water injection operations. *Desalination* **2007,** *208* (1), 159-168.

4.   Lim, D.; Gruehagen, H., Subsea Separation and Boosting—An Overview of Ongoing Projects. In *Asia Pacific Oil and Gas Conference & Exhibition*, Society of Petroleum Engineers: Jakarta, Indonesia, 2009.

5.   Bringedal, B.; Ingebretsen, T.; Haugen, K., Subsea Separation and Reinjection of Produced Water. In *Offshore Technology Conference*, Offshore Technology Conference: Houston, Texas, 1999.

6.   Chesters, A. K., The modelling of coalescence processes in fluid-liquid dispersions: a review of current understanding. *Chem. Eng. Res. Des.* **1991,** *69* (A4), 259-270.

7.   Kourio, M. J.; Gourdon, C.; Casamatta, G., Study of drop-interface coalescence: Drainage time measurement. *Chemical Engineering & Technology* **1994,** *17* (4), 249-254.

8.   Podgórska, W., Influence of Dispersed Phase Viscosity on Drop Coalescence in Turbulent Flow. *Chem. Eng. Res. Des.* **2007,** *85* (5), 721-729.

9.   Kamp, J.; Kraume, M., Influence of drop size and superimposed mass transfer on coalescence in liquid/liquid dispersions – Test cell design for single drop investigations. *Chem. Eng. Res. Des.* **2014,** *92* (4), 635-643.

10.   Bhardwaj, A.; Hartland, S., Kinetics of coalescence of water droplets in water-in-crude oil emulsions. *J. Dispersion Sci. Technol.* **1994,** *15* (2), 133-146.

11.   Frising, T.; Noïk, C.; Dalmazzone, C., The Liquid/Liquid Sedimentation Process: From Droplet Coalescence to Technologically Enhanced Water/Oil Emulsion Gravity Separators: A Review. *J. Dispersion Sci. Technol.* **2006,** *27* (7), 1035-1057.

12.   Bresciani, A. E.; Alves, R. M. B.; Nascimento, C. A. O., Coalescence of water droplets in crude oil emulsions: Analytical solution. *Chem. Eng. Technol.* **2010,** *33* (2), 237-243.

13.   Opedal, N. v. d. T.; Kralova, I.; Lesaint, C.; Sjöblom, J., Enhanced Sedimentation and Coalescence by Chemicals on Real Crude Oil Systems. *Energy Fuels* **2011,** *25* (12), 5718-5728.

14.   Sterling Jr, M. C.; Ojo, T.; Autenrieth, R. L.; Bonner, J. S.; Page, C. A.; Ernest, A. N. S. In *Coalescence kinetics of dispersed crude oil in a laboratory reactor*, Environment Canada Arctic and Marine Oil Spill Program Technical Seminar (AMOP) Proceedings, 2002; pp 741-753.

15.   Gaweł, B.; Lesaint, C.; Bandyopadhyay, S.; Øye, G., Role of Physicochemical and Interfacial Properties on the Binary Coalescence of Crude Oil Drops in Synthetic Produced Water. *Energy Fuels* **2015,** *29* (2), 512-519.

16.   Poteau, S.; Argillier, J.-F.; Langevin, D.; Pincet, F.; Perez, E., Influence of pH on Stability and Dynamic Properties of Asphaltenes and Other Amphiphilic Molecules at the Oil–Water Interface†. *Energy Fuels* **2005,** *19* (4), 1337-1341.

17.   Sjöblom, J.; Marit-Helen, E.; Wanzhen, L.; Xiaoli, Y., Film Properties of Asphaltenes and Resins. In *Encyclopedic Handbook of Emulsion Technology*, CRC Press: 2001; pp 525-540.

18.   Havre, T. E.; Sjöblom, J.; Vindstad, J. E., Oil/Water-Partitioning and Interfacial Behavior of Naphthenic Acids. *J. Dispersion Sci. Technol.* **2003,** *24* (6), 789-801.

19.   Bertheussen, A.; Simon, S.; Sjöblom, J., Equilibrium partitioning of naphthenic acids and bases and their consequences on interfacial properties. *Colloids Surf. Physicochem. Eng. Aspects* **2017,** *529* (Supplement C), 45-56.

20.   Eftekhardadkhah, M.; Kløcker, K. N.; Trapnes, H. H.; Gaweł, B.; Øye, G., Composition and Dynamic Adsorption of Crude Oil Components Dissolved in Synthetic Produced Water at Different pH Values. *Ind. Eng. Chem. Res.* **2016,** *55* (11), 3084-3090.

21.   Krebs, T.; Schroën, K.; Boom, R., Coalescence dynamics of surfactant-stabilized emulsions studied with microfluidics. *Soft Matter* **2012,** *8* (41), 10650-10657.

22.   Krebs, T.; Schroën, C. G. P. H.; Boom, R. M., Coalescence kinetics of oil-in-water emulsions studied with microfluidics. *Fuel* **2013,** *106*, 327-334.

23.   Mazutis, L.; Griffiths, A. D., Selective droplet coalescence using microfluidic systems. *Lab Chip* **2012,** *12* (10), 1800-6.

24.   Tan, Y.-C.; Ho, Y. L.; Lee, A. P., Droplet coalescence by geometrically mediated flow in microfluidic channels. *Microfluid. Nanofluid.* **2007,** *3* (4), 495-499.

25.   Baret, J.-C.; Kleinschmidt, F.; El Harrak, A.; Griffiths, A. D., Kinetic Aspects of Emulsion Stabilization by Surfactants: A Microfluidic Analysis. *Langmuir* **2009,** *25* (11), 6088-6093.

26.   Zagnoni, M.; Cooper, J. M., On-chip electrocoalescence of microdroplets as a function of voltage, frequency and droplet size. *Lab Chip* **2009,** *9* (18), 2652-2658.

27.   Fisher, R.; Shah, M. K.; Eskin, D.; Schmidt, K.; Singh, A.; Molla, S.; Mostowfi, F., Equilibrium gas-oil ratio measurements using a microfluidic technique. *Lab Chip* **2013,** *13* (13), 2623-33.

28.   Alabi, O. O.; Bowden, S. A.; Parnell, J., Simultaneous and rapid asphaltene and TAN determination for heavy petroleum using an H-cell. *Analytical Methods* **2014,** *6* (11), 3651-3660.

29.   Floquet, C. F. A.; Sieben, V. J.; MacKay, B. A.; Mostowfi, F., Determination of boron concentration in oilfield water with a microfluidic ion exchange resin instrument. *Talanta* **2016,** *154*, 304-311.

30.   Nowbahar, A.; Whitaker, K. A.; Schmitt, A. K.; Kuo, T.-C., Mechanistic Study of Water Droplet Coalescence and Flocculation in Diluted Bitumen Emulsions with Additives Using Microfluidics. *Energy Fuels* **2017**.

31.   Won, J. Y.; Krägel, J.; Makievski, A. V.; Javadi, A.; Gochev, G.; Loglio, G.; Pandolfini, P.; Leser, M. E.; Gehin-Delval, C.; Miller, R., Drop and bubble micro manipulator (DBMM)—A unique tool for mimicking processes in foams and emulsions. *Colloids Surf. Physicochem. Eng. Aspects* **2014,** *441*, 807-814.

32.   Dudek, M.; Muijlwijk, K.; Schroen, C. G. P. H.; Øye, G., The effect of dissolved gas on coalescence of oil drops studied with microfluidics. *J. Colloid Interface Sci.* **2018,** *528*, 166-173.

33.   Dudek, M.; Kancir, E.; Øye, G., Influence of the Crude Oil and Water Compositions on the Quality of Synthetic Produced Water. *Energy Fuels* **2017,** *31* (4), 3708-3716.

34.   *Produced Water: Technological/Environmental Issues and Solutions*. Springer US: 1992; Vol. 46, p 632.

35.   Anna, S. L., Droplets and Bubbles in Microfluidic Devices. *Annual Review of Fluid Mechanics* **2016,** *48* (1), 285-309.

36.   Hansen, E. W. M.; Rørtveit, G. J., Numerical Simulation of Fluid Mechanisms and Separation Behavior in Offshore Gravity Separators. In *Emulsions and Emulsion Stability*, Sjöblom, J., Ed. Taylor & Francis: Boca Raton, FL, 2006; Vol. 132.

37.   Brown, C. E.; Neustadter, E. L., The Wettability of Oil/Water/Silica Systems With Reference to Oil Recovery. **1980**.

38.   Arla, D.; Sinquin, A.; Palermo, T.; Hurtevent, C.; Graciaa, A.; Dicharry, C., Influence of pH and Water Content on the Type and Stability of Acidic Crude Oil Emulsions. *Energy Fuels* **2007,** *21* (3), 1337-1342.

39.   Nenningsland, A. L.; Simon, S.; Sjöblom, J., Surface Properties of Basic Components Extracted from Petroleum Crude Oil. *Energy Fuels* **2010,** *24* (12), 6501-6505.

40.   Hutin, A.; Argillier, J.-F.; Langevin, D., Mass Transfer between Crude Oil and Water. Part 1: Effect of Oil Components. *Energy Fuels* **2014,** *28* (12), 7331-7336.

41.   Hurtevent, C.; Rousseau, G.; Bourrel, M.; Brocart, B., Production Issues of Acidic Petroleum Crude Oils. In *Emulsions and Emulsion Stability*, Sjöblom, J., Ed. Taylor & Francis Group LLC: Boca Raton, FL, 2006; pp 477-516.

42.   Sjöblom, J.; Simon, S.; Xu, Z., The chemistry of tetrameric acids in petroleum. *Adv. Colloid Interface Sci.* **2014,** *205*, 319-338.

43.   Mapolelo, M. M.; Rodgers, R. P.; Blakney, G. T.; Yen, A. T.; Asomaning, S.; Marshall, A. G., Characterization of naphthenic acids in crude oils and naphthenates by electrospray ionization FT-ICR mass spectrometry. *Int. J. Mass spectrom.* **2011,** *300* (2), 149-157.

44.   Havre, T. E., Near-IR spectroscopy as a method for studying the formation of calcium naphthenate. *Colloid. Polym. Sci.* **2004,** *282* (3), 270-279.

45.   Tichelkamp, T.; Teigen, E.; Nourani, M.; Øye, G., Systematic study of the effect of electrolyte composition on interfacial tensions between surfactant solutions and crude oils. *Chem. Eng. Sci.* **2015,** *132*, 244-249.

46.   Dyer, S. J.; Graham, G. M.; Arnott, C., Naphthenate Scale Formation - Examination of Molecular Controls in Idealised Systems. In *International Symposium on Oilfield Scale*, Society of Petroleum Engineers: Aberdeen, United Kingdom, 2003.

47.   Brandal, Ø.; Sjöblom, J., Interfacial Behavior of Naphthenic Acids and Multivalent Cations in Systems with Oil and Water. II: Formation and Stability of Metal Naphthenate Films at Oil-Water Interfaces. *J. Dispersion Sci. Technol.* **2005,** *26* (1), 53-58.

48.   Parra-Barraza, H.; Hernández-Montiel, D.; Lizardi, J.; Hernández, J.; Herrera Urbina, R.; Valdez, M. A., The zeta potential and surface properties of asphaltenes obtained with different crude oil/n-heptane proportions☆. *Fuel* **2003,** *82* (8), 869-874.

49.   Wolstenholme, G. A.; Schulman, J. H., Metal-monolayer interactions in aqueous systems. Part I.-The interaction of monolayers of long-chain polar compounds with metal ions in the underlying solution. *Trans. Faraday Society* **1950,** *46* (0), 475-487.

50.   Mullins, O. C., The Modified Yen Model. *Energy Fuels* **2010,** *24* (4), 2179-2207.

51.   Georgieva, D.; Schmitt, V.; Leal-Calderon, F.; Langevin, D., On the Possible Role of Surface Elasticity in Emulsion Stability. *Langmuir* **2009,** *25* (10), 5565-5573.

52.   Angle, C. W.; Hua, Y., Dilational Interfacial Rheology for Increasingly Deasphalted Bitumens and n-C5 Asphaltenes in Toluene/NaHCO3 Solution. *Energy Fuels* **2012,** *26* (10), 6228-6239.

53.   Nenningsland, A. L.; Simon, S.; Sjöblom, J., Influence of Interfacial Rheological Properties on Stability of Asphaltene-Stabilized Emulsions. *J. Dispersion Sci. Technol.* **2014,** *35* (2), 231-243.

54.   Bertheussen, A.; Simon, S. C.; Sjoblom, J., Equilibrium partitioning of naphthenic acid mixture part 1: Commercial naphthenic acid mixture. *Energy Fuels* **2018**.

55.   Hansen, B. R.; Davies, S. H., Review of potential technologies for the removal of dissolved components from produced water. *Chem. Eng. Res. Des.* **1994,** *72* (A2), 176-188.

56.   Rogers, V. V.; Wickstrom, M.; Liber, K.; MacKinnon, M. D., Acute and Subchronic Mammalian Toxicity of Naphthenic Acids from Oil Sands Tailings. *Toxicol. Sci.* **2002,** *66* (2), 347-355.

57.   Eftekhardadkhah, M.; Reynders, P.; Øye, G., Dynamic adsorption of water soluble crude oil components at air bubbles. *Chem. Eng. Sci.* **2013,** *101*, 359-365.

58.   Eftekhardadkhah, M.; Øye, G., Dynamic Adsorption of Organic Compounds Dissolved in Synthetic Produced Water at Air Bubbles: The Influence of the Ionic Composition of Aqueous Solutions. *Energy Fuels* **2013,** *27* (9), 5128-5134.

59.   Eftekhardadkhah, M.; Aanesen, S. V.; Rabe, K.; Øye, G., Oil Removal from Produced Water during Laboratory- and Pilot-Scale Gas Flotation: The Influence of Interfacial Adsorption and Induction Times. *Energy Fuels* **2015,** *29* (11), 7734-7740.

60.   Spiecker, P. M.; Gawrys, K. L.; Trail, C. B.; Kilpatrick, P. K., Effects of petroleum resins on asphaltene aggregation and water-in-oil emulsion formation. *Colloids Surf. Physicochem. Eng. Aspects* **2003,** *220* (1), 9-27.

61.   Murgich, J.; Strausz, O. P., Molecular Mechanics of Aggregates of Asphaltenes and Resins of the Athabasca Oil. *Pet. Sci. Technol.* **2001,** *19* (1-2), 231-243.

62.   Schorling, P. C.; Kessel, D. G.; Rahimian, I., Influence of the crude oil resin/asphaltene ratio on the stability of oil/water emulsions. *Colloids Surf. Physicochem. Eng. Aspects* **1999,** *152* (1), 95-102.

63.   Strassner, J. E., Effect of pH on Interfacial Films and Stability of Crude Oil-Water Emulsions. **1968**.

64.   Groothuis, H.; Zuiderweg, F. J., Influence of mass transfer on coalescence of drops. *Chem. Eng. Sci.* **1960,** *12* (4), 288-289.

65.   Chevaillier, J. P.; Klaseboer, E.; Masbernat, O.; Gourdon, C., Effect of mass transfer on the film drainage between colliding drops. *J. Colloid Interface Sci.* **2006,** *299* (1), 472-485.

66.   Kopriwa, N.; Buchbender, F.; Ayesterán, J.; Kalem, M.; Pfennig, A., A Critical Review of the Application of Drop-Population Balances for the Design of Solvent Extraction Columns: I. Concept of Solving Drop-Population Balances and Modelling Breakage and Coalescence. *Solvent Extr. Ion Exch.* **2012,** *30* (7), 683-723.

67.   Spildo, K.; Høiland, H., Interfacial Properties and Partitioning of 4-Heptylbenzoic Acid between Decane and Water. *J. Colloid Interface Sci.* **1999,** *209* (1), 99-108.

68.   Al-Besharah, J. M.; Akashah, S. A.; Mumford, C. J., The effect of temperature and pressure on the viscosities of crude oils and their mixtures. *Industrial & Engineering Chemistry Research* **1989,** *28* (2), 213-221.

69.   Karnanda, W.; Benzagouta, M. S.; AlQuraishi, A.; Amro, M. M., Effect of temperature, pressure, salinity, and surfactant concentration on IFT for surfactant flooding optimization. *Arabian Journal of Geosciences* **2013,** *6* (9), 3535-3544.

70.   Vieira, L. C.; Buchuid, M. B.; Lucas, E. F., Effect of Pressure on the Crystallization of Crude Oil Waxes. I. Selection of Test Conditions by Microcalorimetry. *Energy Fuels* **2010,** *24* (4), 2208-2212.

71.   Golkari, A.; Riazi, M., *Experimental Investigation of Miscibility Conditions of Dead and Live Asphaltenic Crude Oil-CO₂ Systems*. 2016; Vol. 7.